

Prediction of Giant Spin Motive Force due to Rashba Spin-Orbit Coupling

Kyoung-Whan Kim¹, Jung-Hwan Moon², Kyung-Jin Lee², and Hyun-Woo Lee¹

¹*PCTP and Department of Physics, Pohang University of Science and Technology, Pohang, 790-784, Korea*

²*Department of Materials Science and Engineering, Korea University, Seoul, 136-701, Korea*

(Dated: April 7, 2018)

Magnetization dynamics in a ferromagnet can induce a spin-dependent electric field through spin motive force. Spin current generated by the spin-dependent electric field can in turn modify the magnetization dynamics through spin-transfer torque. While this feedback effect is usually weak and thus ignored, we predict that in Rashba spin-orbit coupling systems with large Rashba parameter α_R , the coupling generates the spin-dependent electric field $[\pm(\alpha_R m_e/e\hbar)(\hat{\mathbf{z}} \times \partial\mathbf{m}/\partial t)]$, which can be large enough to modify the magnetization dynamics significantly. This effect should be relevant for device applications based on ultrathin magnetic layers with strong Rashba spin-orbit coupling.

Similar to the mutual induction between electric and magnetic fields through the Faraday and Maxwell's laws, spin current and magnetization induce the dynamics of each other in magnetic systems through spin-transfer torque (STT) [1–4] and spin motive force (SMF) [5–7]. Through many years of extensive study [3, 4], it has been demonstrated that STT is a powerful tool to induce the magnetization dynamics in ferromagnetic nanostructures. In contrast, SMF has received much less attention [8–10] since SMF is very weak and thus inefficient to generate the spin current.

In this Letter, we demonstrate that SMF can be orders of magnitude enhanced in systems with strong Rashba spin-orbit coupling (RSOC). RSOC arises generically when structural inversion symmetry is broken [11]. Recent experiments on ultrathin (~ 1 nm) ferromagnetic layers with the strong structural inversion asymmetry (such as Pt/Co/AlO_x [12, 13]) observed large effective magnetic fields predicted by RSOC theories [14, 15]. A thin ferromagnetic layer in contact with topological insulators [16, 17] may also have strong RSOC. In such magnetic systems, magnetization dynamics can induce large spin current through SMF, and this spin current can in turn modify the magnetization dynamics through STT. Thus even for *purely magnetic-field-driven* magnetization dynamics, STT can have sizable magnitude because of large spin current generated through SMF. We also propose a SMF-based method to measure the strength of RSOC in magnetic systems. This method allows for unambiguous distinction between RSOC effects and other effects [18], which may be difficult to distinguish through other methods. Thus SMF can also be a useful tool to quantify RSOC.

RSOC can be described by the Rashba Hamiltonian H_R [11],

$$H_R = \frac{\alpha_R}{\hbar}(\boldsymbol{\sigma} \times \mathbf{p}) \cdot \hat{\mathbf{z}} = \frac{\alpha_R}{\hbar}(\sigma_x p_y - \sigma_y p_x), \quad (1)$$

where the vectors $\boldsymbol{\sigma}$ and \mathbf{p} are the Pauli matrix and the momentum, respectively. $\hat{\mathbf{z}}$ is the unit vector along the inversion symmetry breaking direction (perpendicular to ferromagnetic layer), and α_R is the Rashba constant. The total Hamiltonian H of a conduction electron

then becomes $H_0 + H_R$, where $H_0 = \mathbf{p}^2/2m_e - J_{\text{ex}}\boldsymbol{\sigma} \cdot \mathbf{m}$. Here m_e is effective mass of conduction electrons, J_{ex} (< 0) is the exchange coupling energy, and \mathbf{m} is the unit vector along the local magnetization, which is in general time- and position-dependent. An insight into the RSOC effect on SMF can be gained from the velocity operator $\mathbf{v} = [\mathbf{r}, H]/i\hbar = \mathbf{p}/m_e + \mathbf{v}_{\text{an}}$, where the anomalous velocity $\mathbf{v}_{\text{an}} = [\mathbf{r}, H_R]/i\hbar = \alpha_R \hat{\mathbf{z}} \times \boldsymbol{\sigma}/\hbar$ arises due to RSOC. When the exchange energy is sufficiently larger than RSOC, $\boldsymbol{\sigma}$ for majority (minority) electrons will be almost anti-parallel (parallel) to \mathbf{m} . It is then evident that the magnetization dynamics $\partial\mathbf{m}/\partial t$ induces the acceleration $d\mathbf{v}_{\text{an}}/dt$ and the effective electric field $-(m_e/e)d\mathbf{v}_{\text{an}}/dt$. This heuristic calculation results in the RSOC contribution to the spin-dependent electric field $\mathbf{E}_{\pm}^{\text{RSOC}}$,

$$\mathbf{E}_{\pm}^{\text{RSOC}} = \pm\alpha_R \frac{m_e}{e\hbar} \left(\hat{\mathbf{z}} \times \frac{\partial\mathbf{m}}{\partial t} \right), \quad (2)$$

where \pm applies to the majority and minority electrons, respectively. The total spin-dependent electric field \mathbf{E}'_{\pm} then becomes $\mathbf{E}_{\pm} + \mathbf{E}_{\pm}^{\text{RSOC}}$, where

$$\mathbf{E}_{\pm} = \pm \sum_i \hat{\mathbf{x}}_i \frac{\hbar}{2e} \left(\frac{\partial\mathbf{m}}{\partial t} \times \frac{\partial\mathbf{m}}{\partial x_i} \right) \cdot \mathbf{m} \quad (3)$$

represents the conventional spin-dependent electric field examined in previous literatures [7, 19] in the absence of RSOC. For more rigorous derivation of Eq. (2), we may adopt the calculation scheme in Ref. [6]. One first diagonalizes the exchange coupling term $-J_{\text{ex}}\boldsymbol{\sigma} \cdot \mathbf{m}$ by introducing the unitary operator $U^\dagger = e^{i\theta\sigma_y/2} e^{i\phi\sigma_z/2}$, where the Euler angles (θ, ϕ) are defined by spatio-temporal profile of $\mathbf{m} = (\sin\theta \cos\phi, \sin\theta \sin\phi, \cos\theta)$. The transformed Hamiltonian $H' \equiv U^\dagger H U - i\hbar U^\dagger \partial_t U$ becomes $H' = (\mathbf{p} + e\mathbf{A}')^2/2m_e - J_{\text{ex}}\sigma_z - eA'_0$, where \mathbf{m} is rotated to $(0, 0, 1)$ and the exchange coupling term is diagonal, $-J_{\text{ex}}\sigma_z$. Information on SMF is now stored in vector and scalar potentials \mathbf{A}' and A'_0 given by $\mathbf{A}' = -(i\hbar/e)U^\dagger \nabla U - (\alpha_R m_e/e\hbar)U^\dagger(\boldsymbol{\sigma} \times \hat{\mathbf{z}})U$ and $A'_0 = (i\hbar/e)U^\dagger \partial_t U + \alpha_R^2 m_e/e\hbar^2$. Recalling that spins tend to

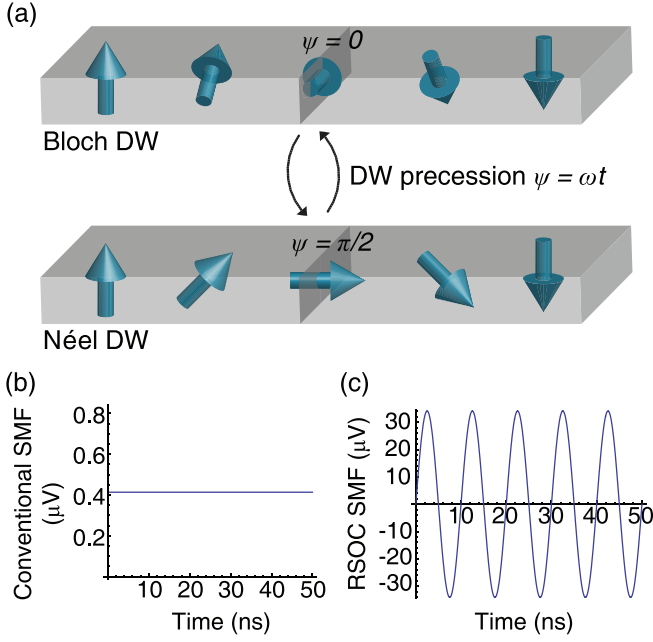


FIG. 1: (color online) Voltage produced by a precessing DW in a nanowire. For simplicity, the DW motion along the nanowire is assumed to be suppressed by a notch in the nanowire. (a) Schematic structure of DW. DW is assumed to precess and change its structure periodically between the Bloch DW ($\psi = 0$ or π) and the Néel DW ($\psi = \pi/2$ or $3\pi/2$) with $\omega = d\psi/dt = 2\pi \times 100$ MHz. (b) Voltage between the two ends of the nanowire due to \mathbf{E}_{\pm} . This voltage does not depend on time t in this particular case since the t -dependences of \mathbf{m} , $\partial\mathbf{m}/\partial t$, and $\partial\mathbf{m}/\partial x_i$ mutually cancel in Eq. (3). The voltage magnitude is comparable to the value reported in Ref. [8]. (c) Voltage due to $\mathbf{E}_{\pm}^{\text{RSOC}}$, which oscillates with t . Here $\alpha_R = 10^{-10}$ eV·m [12], $P = 1$, and the DW width of 20 nm are assumed.

be parallel or anti-parallel to $\mathbf{m} = (0, 0, 1)$, we may retain only diagonal components of the potentials for leading order calculation. Then the conventional formula $-\partial_t \mathbf{A}' - \nabla A'_0$ determines the total electric field \mathbf{E}'_{\pm} (\mathbf{E}'_{-}) for the majority ($\sigma_z = -1$) (minority $\sigma_z = +1$) electrons. This calculation reproduces Eqs. (2) and (3).

We estimate the relative magnitude of $\mathbf{E}_{\pm}^{\text{RSOC}}$ with respect to \mathbf{E}_{\pm} ; $\mathbf{E}_{\pm}^{\text{RSOC}}$ is of the order of $(\alpha_R m_e / e\hbar)\omega$, where ω is the characteristic angular frequency of the magnetization dynamics, and \mathbf{E}_{\pm} is of the order of $(\hbar/e)(\omega/L)$, where L is the characteristic length of a magnetic structure [such as domain wall (DW) width] producing \mathbf{E}_{\pm} . The relative ratio becomes $\alpha_R m_e L / \hbar^2 \approx \alpha_R L \times 10^{38}$ ($\text{kg}/\text{J}^2 \cdot \text{s}^2$) for $m_e = 9.1 \times 10^{-31}$ kg. For the value $\alpha_R = 10^{-10}$ eV·m reported for Pt/Co(0.6 nm)/AlO_x [12] and for $L = 20$ nm, this ratio becomes about 30. Thus $\mathbf{E}_{\pm}^{\text{RSOC}}$ can be more than an order of magnitude larger than \mathbf{E}_{\pm} .

For magnetic materials with nonzero spin polarization P , spin-dependent electric fields can be measured through conventional electric voltage measurement [9].

Figure 1 compares electrical voltages produced by a precessing DW in a nanowire. The voltage due to $\mathbf{E}_{\pm}^{\text{RSOC}}$ [Fig. 1(c)] exhibits time-dependence different from that due to \mathbf{E}_{\pm} [Fig. 1(b)] because of the functional form difference between Eqs. (2) and (3). Note that the oscillation amplitude in Fig. 1(c) is about 80 times larger than the dc value in Fig. 1(b).

In regard to the value of α_R , 10^{-10} eV·m for Pt/Co(0.6 nm)/AlO_x [12] is not exceptional. The α_R value in the range $(0.4 - 3) \times 10^{-10}$ eV·m was reported by photoelectron spectroscopy measurements [20, 21] for a thin nonmagnetic metal layer in contact with a heavy atomic element layer. Since magnetism does not suppress α_R , its value can be in a similar range for proper combinations of a thin magnetic layer in contact with a heavy atomic element layer. A recent effective field measurement result [22] for Ta/CoFeB(1 nm)/MgO implies $\alpha_R \approx 0.2 \times 10^{-10}$ eV·m, which falls close to the common range. For this particular multilayer, it was suggested [22] that the contact with the oxide layer MgO may also be an important source of α_R . Still another candidate system is a thin magnetic layer in contact with topological insulators. For instance, BiTeI has a large bulk RSOC with $\alpha_R = 3.8 \times 10^{-10}$ eV·m [16] and was predicted [17] to become a topological insulator under pressure.

Large spin-dependent electric field implies large spin current. The spin current density generated by SMF becomes $\mathbf{J}_s^{\text{SMF}} = \sigma_{\uparrow}(\mathbf{E}_{+} + \mathbf{E}_{+}^{\text{RSOC}}) - \sigma_{\downarrow}(\mathbf{E}_{-} + \mathbf{E}_{-}^{\text{RSOC}}) = \sigma_c(\mathbf{E}_{+} + \mathbf{E}_{+}^{\text{RSOC}})$ [23], where $\sigma_{\uparrow(\downarrow)}$ is the longitudinal electrical conductivity of majority (minority) electrons and $\sigma_c = \sigma_{\uparrow} + \sigma_{\downarrow}$. Since $\mathbf{E}_{+}^{\text{RSOC}}$ is much larger than \mathbf{E}_{+} and $\mathbf{E}_{\pm}^{\text{RSOC}}$ is perpendicular to $\hat{\mathbf{z}}$ [Eq. (2)], $\mathbf{J}_s^{\text{SMF}}$ flows *within* a magnetic layer. Then for a typical in-plane charge conductivity $\sigma_c = 10^7 \Omega^{-1} \cdot \text{m}^{-1}$ of metallic ferromagnetic layers and $\alpha_R = (0.2 - 3) \times 10^{-10}$ eV·m, $\mathbf{J}_s^{\text{SMF}}$ has magnitude $(1.8 - 27)\tau^{-1}$ A·s/m², where τ is the characteristic time scale of magnetization dynamics. For fast DW motion with speed 400 m/s [24], we find that $|\mathbf{J}_s^{\text{SMF}}|$ goes up to $(0.18 - 2.7) \times 10^{11}$ A/m² near the DW center of width 20 nm. Thus RSOC allows SMF to generate large spin current density for fast magnetization dynamics.

Large $\mathbf{J}_s^{\text{SMF}}$ generated by magnetization dynamics implies that magnetization dynamics *itself* can be significantly modified by $\mathbf{J}_s^{\text{SMF}}$ through STT. Next we examine this feedback effect. In conventional situations where SMF is negligible, the magnetization dynamics is described by the Landau-Lifshitz-Gilbert (LLG) equation, $\partial\mathbf{m}/\partial t = -\gamma\mathbf{m} \times \mathbf{H}_{\text{eff}} + \alpha_G \mathbf{m} \times \partial\mathbf{m}/\partial t + \mathbf{T}(\mathbf{J}_s)$, where \mathbf{T} represents the STT and depends on externally supplied spin current density \mathbf{J}_s . Here γ is the gyromagnetic ratio, α_G is the Gilbert damping parameter, and \mathbf{H}_{eff} is the sum of an external magnetic field and effective magnetic fields due to magnetic anisotropy and magnetic exchange energy. To examine the feedback effect, one simply needs

to replace $\mathbf{T}(\mathbf{J}_s)$ by $\mathbf{T}(\mathbf{J}_s + \mathbf{J}_s^{\text{SMF}}) = \mathbf{T}(\mathbf{J}_s) + \mathbf{T}(\mathbf{J}_s^{\text{SMF}})$ to obtain the modified LLG equation,

$$\frac{\partial \mathbf{m}}{\partial t} = -\gamma \mathbf{m} \times \mathbf{H}_{\text{eff}} + \alpha_G \mathbf{m} \times \frac{\partial \mathbf{m}}{\partial t} + \mathbf{T}(\mathbf{J}_s) + \mathbf{T}(\mathbf{J}_s^{\text{SMF}}). \quad (4)$$

Note that STT \mathbf{T} now has two spin current sources, \mathbf{J}_s and $\mathbf{J}_s^{\text{SMF}}$. Thus even when there is no externally supplied spin current ($\mathbf{J}_s = 0$), STT still affects the magnetization dynamics as long as $\mathbf{J}_s^{\text{SMF}}$ is not zero. Therefore STT becomes relevant even for *purely field-driven* magnetization dynamics.

To gain an insight into roles of the feedback STT $\mathbf{T}(\mathbf{J}_s^{\text{SMF}})$, we express it in the following form,

$$\mathbf{T}(\mathbf{J}_s^{\text{SMF}}) = \mathbf{m} \times \mathcal{D} \cdot \frac{\partial \mathbf{m}}{\partial t}. \quad (5)$$

This form is natural since \mathbf{T} is orthogonal to \mathbf{m} [thus $\mathbf{T}(\mathbf{J}_s^{\text{SMF}}) = \mathbf{m} \times (\text{function of } \mathbf{J}_s^{\text{SMF}})$] and $\mathbf{J}_s^{\text{SMF}}$ is proportional to $\partial \mathbf{m} / \partial t$ [thus (function of $\mathbf{J}_s^{\text{SMF}}) = \mathcal{D} \cdot \partial \mathbf{m} / \partial t$]. Here \mathcal{D} will depend on \mathbf{m} and be a 3×3 matrix in general. Although \mathcal{D} is not a constant, the structural similarity between Eq. (5) and the Gilbert damping torque $\alpha_G \mathbf{m} \times \partial \mathbf{m} / \partial t$ implies that \mathcal{D} may be interpreted as a correction to the Gilbert damping parameter α_G . Thus roles of the feedback STT can be analyzed by using this damping correction picture.

After explicit calculation, we find that the matrix elements of the 3×3 matrix \mathcal{D} are given by

$$\mathcal{D}_{ij} = \eta \sum_k (X_{ki} + \tilde{\alpha}_R \epsilon_{3ki}) (X_{kj} + \tilde{\alpha}_R \epsilon_{3kj}), \quad (6)$$

where $X_{ki} = (\mathbf{m} \times \partial \mathbf{m} / \partial x_k)_i$, $\eta = \mu_B \hbar \sigma_c / 2e^2 M_s$, $\tilde{\alpha}_R = 2\alpha_R m_e / \hbar^2$, $\mu_B (> 0)$ is the Bohr magneton, M_s is the saturation magnetization, and ϵ_{ijk} is the Levi-Civita permutation symbol ($\epsilon_{123} = 1$). To derive Eq. (6), we simply combine the spin-dependent electric field equations [Eqs. (2) and (3)] with known contributions to STT. To be specific, the adiabatic STT contribution [$\propto (\mathbf{J}_s \cdot \nabla) \mathbf{m}$] and the field-like STT contribution [$\propto \alpha_R \mathbf{m} \times (\hat{\mathbf{z}} \times \mathbf{J}_s)$] [14, 15] are taken into account in the calculation whereas the nonadiabatic STT contribution and recently discovered Slonczewski-like STT contribution [25–27] are ignored since the latter two contributions are smaller than the former two.

The importance of the feedback STT can be estimated from the relative magnitude of \mathcal{D} with respect to α_G . Here α_G includes all contributions other than the SMF contribution. The intrinsic bulk Gilbert damping parameter is of the order of 0.01 for typical metallic ferromagnets. In a thin magnetic layer, this intrinsic value is enhanced by the conventional spin pumping mechanism [28, 29] and the enhanced value is estimated to $0.1/d_F$ (nm), which is 0.1 for thin magnetic layer of thickness $d_F = 1$ nm. Thus for the feedback effect to be a relevant factor for the magnetization dynamics of a

thin magnetic layer, \mathcal{D} should be comparable to or larger than 0.1. When RSOC is absent ($\tilde{\alpha}_R = 0$), \mathcal{D} reduces to the result in Ref. [19] and is of the order of η/L^2 . For $\sigma_c = 10^7 \Omega^{-1} \cdot \text{m}^{-1}$, $M_s = 10^6$ A/m and $L = 20$ nm, η is 0.2 nm^2 and η/L^2 is 0.0005. Thus except for special situations with $L \lesssim 1$ nm, \mathcal{D} becomes much smaller than 0.1 and the feedback effect is negligible. When RSOC is strong, on the other hand, the largest contribution to \mathcal{D} arises from the term $\eta \tilde{\alpha}_R^2 \sum_k \epsilon_{3ki} \epsilon_{3kj}$ and thus \mathcal{D} becomes of the order of $\alpha'_G \equiv \eta \tilde{\alpha}_R^2$ [30]. For $\alpha_R = 10^{-10} \text{ eV} \cdot \text{m}$ [12], $\tilde{\alpha}_R$ is 2.6 nm^{-1} and α'_G is 1.4. Since $\alpha'_G \gg \alpha_G$, one of evident effects of the feedback effect is to enhance the effective damping significantly.

For deeper understanding of the feedback effect, however, one should address the detailed structure of the damping matrix \mathcal{D} in Eq. (6). Extensive discussion on implications of the damping matrix structure will be presented elsewhere. Here we present one simple implication contained in the largest contribution $\alpha'_G \sum_k \epsilon_{3ki} \epsilon_{3kj}$, which reduces to $\alpha'_G (\delta_{ij} - \delta_{3i} \delta_{3j})$ after simple algebra. This contribution makes the effective damping anisotropic since $\sum_j (\delta_{ij} - \delta_{3i} \delta_{3j}) (\partial \mathbf{m} / \partial t)_j$ becomes $(\partial \mathbf{m} / \partial t)_i$ when $\partial \mathbf{m} / \partial t$ is perpendicular to $\hat{\mathbf{z}}$ -direction, and vanishes when $\partial \mathbf{m} / \partial t$ is parallel to $\hat{\mathbf{z}}$ -direction. For a magnetic layer with the perpendicular magnetic anisotropy, this damping anisotropy can be tested in experiments by measuring the effective damping in two different ways. When the effective damping is measured by ferromagnetic resonance, $\partial \mathbf{m} / \partial t$ remains essentially perpendicular to $\hat{\mathbf{z}}$ -direction and thus the effective damping becomes $\alpha_G + \alpha'_G$. The effective damping may be measured alternatively by using the relation that the field-driven DW velocity below the Walker-breakdown threshold is inversely proportional to the effective damping. This measurement should produce a smaller effective damping value than the ferromagnetic resonance since $\partial \mathbf{m} / \partial t$ is along the $\pm \hat{\mathbf{z}}$ -direction at the DW center. From a simple calculation based on the Thiele's collective coordinate description [31] of the DW configuration in terms of the DW position and DW tilting angle, we find that the effective damping becomes $\alpha_G + \alpha'_G / 3$. Thus in strong RSOC systems, where $\alpha'_G \gg \alpha_G$, we predict that the effective damping for the ferromagnetic resonance is about factor 3 larger than that for the DW motion. By the way, Ref. [12] determined the effective damping for Pt/Co(0.6 nm)/AlO_x from the field-driven DW motion measurement and found 0.5, which is in reasonable agreement with our prediction $\alpha_G + \alpha'_G / 3 \approx \alpha'_G / 3 \approx 0.5$ for the system.

Figure 2 shows schematically an experimental setup to test the RSOC-enhanced SMF directly. When a *uniformly* magnetized magnetic domain precesses due to external magnetic field $B(t) = B \sin \omega t$, $\mathbf{E}_{\pm}^{\text{RSOC}}$ will generate electric voltages V_x and V_y . Since $\mathbf{E}_{\pm}^{\text{RSOC}}$ is position-independent [Eq. (2)], these voltages should be proportional to the spacing d between electrodes. Also since the

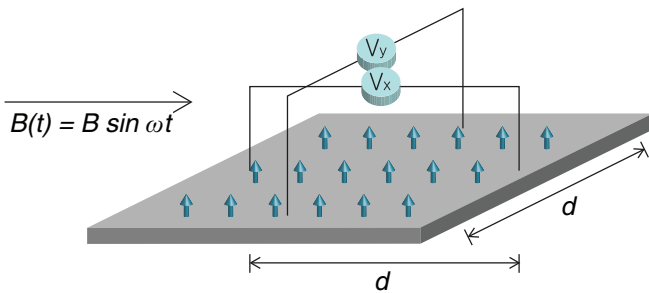


FIG. 2: (color online) Measurement scheme of the RSOC effect on the SMF for a uniformly magnetized layer with the perpendicular magnetic anisotropy.

direction of $\mathbf{E}_{\pm}^{\text{RSOC}}$ rotates within xy -plane as $\partial\mathbf{m}/\partial t$ rotates within xy -plane (due to the perpendicular magnetic anisotropy), the voltages will be oscillatory with the oscillation phases of V_x and V_y different from each other by about 90° . These features are qualitatively different from other effects that may affect this measurement. The conventional spin pumping [28] may also contribute to the electric voltages if the two electrical contacts with the electrodes are not identical, as demonstrated in Ref. [32]. This contribution is however independent of d and thus distinguishable from the RSOC-enhanced SMF contribution. Spin Hall effect in contacts or the neighboring heavy metal layer can also generate a contribution. This spin Hall contribution is however different from the RSOC-enhanced SMF contribution since $\hat{\mathbf{z}} \times \mathbf{m}$ determines the direction of the voltage gradient in case of the spin Hall contribution whereas $\hat{\mathbf{z}} \times \partial\mathbf{m}/\partial t$ does in case of the RSOC-enhanced SMF contribution. Recalling that \mathbf{m} and $\partial\mathbf{m}/\partial t$ are orthogonal to each other, these two contributions differ by the oscillation phase of 90° . A recent experiment [18] demonstrated that in certain experimental situations [33], the spin Hall effect can be very similar to the RSOC effect. The electrical voltage measurement in Fig. 2 can be a very decisive experiment to verify the RSOC-enhanced SMF and also RSOC itself free from such ambiguities. The Rashba constant α_R can be determined from the proportionality constant between the voltages and d .

Lastly two remarks are in order. Firstly, temperature may affect the predicted phenomena. The value of α_R may depend on temperature. But recalling that the reported value of $\alpha_R = 10^{-10}$ eV·m for Pt/Co/AlO_x [12] was obtained at room temperature, we expect that α_R can stay large even at room temperature. Thermal fluctuation of \mathbf{m} is another possible source of the temperature dependence of SMF. Since the fluctuation is not correlated in space and time, it will not affect the SMF voltage measurements in Figs. 1 and 2 significantly. Thus we expect that temperature effects do not modify SMF effects qualitatively. Secondly, though not elaborated here, RSOC gives rise to not only $\mathbf{E}_{\pm}^{\text{RSOC}}$ [Eq. (2)] but also a

spin-dependent magnetic field. Our preliminary calculation indicates that certain types of magnetization dynamics such as DW motion may be accelerated by this effective magnetic field. Further research is required to understand its effects.

In conclusion, we demonstrated that SMF can be orders of magnitudes enhanced in strong RSOC systems. The enhanced SMF is strong enough to modify the magnetization dynamics significantly. RSOC-enhanced SMF may affect performance of various device applications based on ultrathin magnetic layers [24, 33, 34] since RSOC effects tend to get larger in thinner systems. Thus SMF is not a weak effect of purely scientific concern any more but instead a technologically relevant effect that should be taken into account in future studies. As a final remark, during the revision of this manuscript, we were informed that two other groups [35, 36] also obtained Eq. (2).

We gratefully acknowledge M. Stiles for critical comments on the manuscript. We also acknowledge B.-C. Min, S.-Y. Park, and Y. Jo for stimulating discussion. This work was financially supported by the NRF (2009-0084542, 2010-0014109, 2010-0023798, 2011-0028163, 2011-0030784) and BK21. KWK acknowledges the financial support by the NRF (2011-0009278) and TJ Park.

-
- [1] J. C. Slonczewski, *J. Magn. Mag. Mater.* **159**, L1 (1996).
 - [2] L. Berger, *Phys. Rev. B* **54**, 9353 (1996).
 - [3] S. I. Kiselev *et al.*, *Nature* **425**, 380 (2003).
 - [4] K.-J. Lee, A. Deac, O. Redon, J.-P. Nozières, and B. Dieny, *Nature Mater.* **3**, 877 (2004).
 - [5] L. Berger, *Phys. Rev. B* **33**, 1572 (1986).
 - [6] G. E. Volovik, *J. Phys. C* **20**, L83 (1987).
 - [7] S. E. Barnes and S. Maekawa, *Phys. Rev. Lett.* **98**, 246601 (2007).
 - [8] S. A. Yang *et al.*, *Phys. Rev. Lett.* **102**, 067201 (2009).
 - [9] J. Ohe, S. E. Barnes, H.-W. Lee, and S. Maekawa, *Appl. Phys. Lett.* **95**, 123110 (2009).
 - [10] Y. Yamane *et al.*, *Phys. Rev. Lett.* **107**, 236602 (2011).
 - [11] Y. A. Bychkov and E. I. Rashba, *J. Exp. Theor. Phys. Lett.* **39**, 78 (1984).
 - [12] I. M. Miron *et al.*, *Nature Mater.* **9**, 230 (2010).
 - [13] U. H. Pi *et al.*, *Appl. Phys. Lett.* **97**, 162507 (2010).
 - [14] K. Obata and G. Tatara, *Phys. Rev. B* **77**, 214429 (2008).
 - [15] A. Manchon and S. Zhang, *Phys. Rev. B* **78**, 212405 (2008); A. Matos-Abiague and R. L. Rodriguez-Suarez, *Phys. Rev. B* **80**, 094424 (2009).
 - [16] K. Ishizaka *et al.*, *Nature Mater.* **10**, 521 (2011).
 - [17] M. S. Bahramy, B.-J. Yang, R. Arita, and N. Nagaosa, *Nature Commun.* **3**, 679 (2012).
 - [18] L. Liu, O. J. Lee, T. J. Gudmundsen, D. C. Ralph, and R. A. Buhrman, arXiv:1110.6846.
 - [19] S. Zhang and S.-L. Zhang, *Phys. Rev. Lett.* **102**, 086601 (2009).
 - [20] J. Henk, M. Hoesch, J. Osterwalder, A. Ernst, and P. Bruno, *J. Phys.: Condens. Matter* **16**, 7581 (2004).

- [21] C. R. Ast *et al.*, Phys. Rev. Lett. **98**, 186807 (2007).
- [22] T. Suzuki *et al.*, Appl. Phys. Lett. **98**, 142505 (2011).
- [23] The Hall conductivity is ignored since it is orders of magnitude smaller than the longitudinal conductivity. The diffusion contribution is also ignored, which coarsens the spatial-dependence of the spin current density but does not cause qualitative changes [K.-W. Kim, J.-H. Moon, K.-J. Lee, and H.-W. Lee, Phys. Rev. B **84**, 054462 (2011); J. Shibata and H. Kohno, Phys. Rev. B **84**, 184408 (2011)].
- [24] I. M. Miron *et al.*, Nature Mater. **10**, 419 (2011).
- [25] X. Wang and A. Manchon, arXiv:1111.1216; arXiv:1111.5466.
- [26] K.-W. Kim, S.-M. Seo, J. Ryu, K.-J. Lee, and H.-W. Lee, arXiv:1111.3422v2.
- [27] D. A. Pesin and A. H. MacDonald, arXiv:1201.0990.
- [28] Y. Tserkovnyak, A. Brataas, and G. E. W. Bauer, Phys. Rev. Lett. **88**, 117601 (2002).
- [29] Whereas the conventional spin pumping effect arises from the induced spin current *perpendicular* to a magnetic layer, the RSOC-enhanced SMF induces *in-plane* spin current. Thus their contributions to the Gilbert damping enhancement are independent and should be treated separately.
- [30] When a ferromagnet is a good conductor in the diffusive regime, this expression for α'_G agrees with Eq. (2) in M. Hankiewicz, G. Vignale, and Y. Tserkovnyak, Phys. Rev. B **75**, 174434 (2007).
- [31] A. A. Thiele, Phys. Rev. Lett. **30**, 230 (1973).
- [32] M. V. Costache, M. Sladkov, S. M. Watts, C. H. van der Wal, and B. J. van Wees, Phys. Rev. Lett. **97**, 216603 (2006).
- [33] I. M. Miron *et al.*, Nature **476**, 189 (2011).
- [34] S. Ikeda *et al.*, Nature Mater. **9**, 721 (2010).
- [35] Private communications with A. Sakai and H. Kohno.
- [36] Private communications with Y. Yamane, J. Ieda, and S. Maekawa.